

Reduced order modeling and analysis of the human complement system

Adithya Sagar, Wei Dai[#], Mason Minot[#], and Jeffrey D. Varner*

School of Chemical and Biomolecular Engineering

Cornell University, Ithaca NY 14853

Running Title: A reduced order model of complement

To be submitted: *Scientific Reports*

Denotes equal contribution

*Corresponding author:

Jeffrey D. Varner,

Professor, School of Chemical and Biomolecular Engineering,

244 Olin Hall, Cornell University, Ithaca NY, 14853

Email: jdv27@cornell.edu

Phone: (607) 255 - 4258

Fax: (607) 255 - 9166

Abstract

Complement is an important pathway in innate immunity, inflammation, and many disease processes. However, despite its importance, there have been few validated mathematical models of complement activation. In this study, we developed an ensemble of experimentally validated reduced order complement models. We combined ordinary differential equations with logical rules to produce a compact yet predictive complement model. The model, which described the lectin and alternative pathways, was an order of magnitude smaller than comparable models in the literature. We estimated an ensemble of model parameters from *in vitro* dynamic measurements of the C3a and C5a complement proteins. Subsequently, we validated the model on unseen C3a and C5a measurements not used for model training. Despite its small size, the model was surprisingly predictive. Global sensitivity and robustness analysis suggested complement was robust to any single therapeutic intervention. Only dual dual-knockdown of both C3 and C5 consistently reduced C5a formation when all pathways were activated. Taken together, we developed a reduced order complement model that was computationally inexpensive, and could easily be incorporated into pre-existing or new pharmacokinetic models of immune system function. The model described experimental data, and predicted the need for multiple points of therapeutic intervention to disrupt complement activation.

Keywords: Complement system, systems biology, reduced order models, biochemical engineering

1 Introduction

2 Complement is an important pathway in innate immunity. It plays a significant role in
3 inflammation, host defense as well as many disease processes. Complement was dis-
4 covered in the late 1880s where it was found to 'complement' the bactericidal activity of
5 natural antibodies (1). However, research over the past decade has shown that the im-
6 portance of complement extends well beyond innate immunity. For example, complement
7 contributes to tissue homeostasis by inducing tissue repair (2). Complement has also
8 been linked with several diseases including Alzheimers, Parkinson's disease, multiple
9 sclerosis, schizophrenia, rheumatoid arthritis and sepsis (3, 4). Complement plays both
10 positive and negative roles in cancer; attacking tumor cells with altered surface proteins
11 in some cases, while potentially contributing to tumor growth in others (5, 6). Lastly, sev-
12 eral other important biochemical subsystems are integrated with complement including
13 the coagulation cascade, the autonomous nervous system and inflammation (6). Thus,
14 complement is important in a variety of beneficial and potentially harmful functions in the
15 body.

16 The complement cascade involves over 30 soluble and cell surface proteins, receptors
17 and regulators. The molecular connectivity of complement is complex, see the review of
18 Walport (7, 8). The central outputs of complement are the Membrane Attack Complex
19 (MAC), and the inflammatory mediator proteins C3a and C5a. The membrane attack
20 complex, generated during the terminal phase of the response, forms transmembrane
21 channels which disrupt the membrane integrity of targeted cells, leading to cell lysis and
22 death. On the other hand, the C3a and C5a proteins act as a bridge between innate and
23 adaptive immunity, and play an important role in regulating inflammation (5). Complement
24 activation takes places through three pathways: the classical, the lectin binding and the
25 alternate pathways. Each of these pathways involves a different initiator signal which trig-
26 gers downstream events in the complement system. The classical pathway is triggered

27 by antibody recognition of foreign antigens or other pathogens. A multimeric protein com-
28 plex C1 binds to antibody-antigen complexes and undergoes a conformational change,
29 leading to an activated form with proteolytic activity. This activated complex then cleaves
30 soluble complement proteins C4 and C2 into C4a, C4b, C2a and C2b, respectively. The
31 C4a and C2b fragments bind to form the C4bC2a protease, which is also known as the
32 classical C3 convertase. The lectin pathway is initiated through the binding of L-ficolin or
33 Mannose Binding Lectin (MBL) to carbohydrates on the surfaces of bacterial pathogens.
34 These complexes, in combination with the associated mannose-associated serine pro-
35 teases 1 and 2 (MASP-1/2), also cleave C4 and C2, leading to additional classical C3
36 convertase. Thus, the classical and lectin pathways, initiated by the recognition of a for-
37 eign surface, converge at the classical C3 convertase. However, the alternate pathway
38 works differently. The alternate pathway involves a 'tickover' mechanism in which com-
39 plement protein C3 is spontaneously hydrolyzed to form an activated intermediate C3w;
40 C3w recruits factor B and factor D, leading to the formation of C3wBb. C3wBb can cleave
41 C3 into C3a and C3b, where the C3b fragment can further recruit additional factor B and
42 factor D to form C3bBbC3b, which is also known as the alternate C3 convertase (9). The
43 role of classical and alternate C3 convertases is varied. First, C3 convertases encode
44 an amplification loop by cleaving C3 into C3a and C3b; the C3b fragment is then free to
45 form additional alternate C3 convertases, thereby forming a positive feedback loop. Next,
46 C3 convertase activity links complement initiation with the terminal phase of the cascade
47 through the formation of C5 convertases. Both classical and alternate C3 convertases can
48 recruit an additional C3b subunit to form the classical C5 convertase (C4bC2aC3b), and
49 the alternate C5 convertase (C3bBbC3b), respectively. C5 convertases cleave C5 into
50 the C5a and C5b fragments. The C5b fragment, along with the C6, C7, C8 and multiple
51 C9 complement proteins, form the membrane attack complex. On the other hand, both
52 C3a and C5a are important inflammatory signals involved in several responses (7, 8).

Activation of the complement cascade is strongly regulated by many plasma and host cell proteins. The initiation of the classical pathway via complement protein C1 is controlled by the C1 Inhibitor (C1-Inh), a protease inhibitor belonging to the serpin superfamily. C1-Inh irreversibly binds to and deactivates the active subunits of C1, preventing spontaneous fluid phase and chronic activation of complement (10). Regulation of the upstream elements of complement is also achieved through the interaction of the C4 binding protein (C4BP) with C4b, as well as through the interaction of factor H with C3b (11). These regulatory proteins are also capable of binding their respective targets while they are bound in convertase complexes. Membrane cofactor protein (MCP or CD46) possesses a cofactor activity for C4b and C3b, which protects the host from self-activation of complement (12). Decay accelerating factor (DAF or CD55) is also able to recognize and dissociate both C3 and C5 convertases (13). Carboxypeptidase-N, a well known inflammation regulator, cleaves carboxyl-terminal arginines and lysines of the complement proteins C3a, C4a, and C5a rendering them inactive (14). Lastly, the assembly of the MAC complex is inhibited by vitronectin and clusterin in the plasma, and CD59 at the host surface (15, 16). Thus, there are many points of control which influence complement activation across the three activation pathways.

Developing quantitative mathematical models of complement could be crucial to understanding its role in the body. Traditionally, complement models have been formulated as systems of linear or non-linear ordinary differential equations (ODEs). For example, Hirayama et al. modeled the classical complement pathway as a system of linear ODEs (17), while Korotaevskiy and co-workers modeled the classical, lectin and alternate pathways as a system of non-linear ODEs (18). More recently, large mechanistic models of sections of complement have also been proposed. For example, Liu et al. analyzed the formation of the classical and lectin C3 convertases, and the regulatory role of C4BP using a system of 45 non-linear ODEs with 85 parameters (19). Recently, Zewde and co-

79 workers constructed a detailed mechanistic model of the alternative pathway which con-
80 sisted of 107 ODEs and 74 kinetic parameters and delineated the complement response
81 of the host and pathogen (16). However, these previous modeling studies involved little
82 experimental validation. Thus, while these models are undoubtably important theoretical
83 tools, it is unclear if they can describe or quantitatively predict experimentally validated
84 complement dynamics. The central challenge is the estimation of model parameters from
85 experimental data. Unlike other important cascades, such as coagulation for which there
86 are well developed experimental tools and many publicly available data sets, the data for
87 complement is relatively sparse. Missing or incomplete data sets, and limited quantitative
88 data make the identification of mechanistic complement models difficult.

89 In this study, we developed an ensemble of experimentally validated reduced order
90 complement models. The modeling approach combined ordinary differential equations
91 with logical rules to produce a complement model with a limited number of equations and
92 parameters. The reduced order model, which described the lectin and alternative path-
93 ways, consisted of 18 differential equations with 28 parameters. Thus, the model was an
94 order of magnitude smaller and included more pathways than comparable mathematical
95 models in the literature. We estimated an ensemble of model parameters from *in vitro*
96 time series measurements of the C3a and C5a complement proteins. Subsequently, we
97 validated the model on unseen C3a and C5a measurements that were not used for model
98 training. Despite its small size, the model was surprisingly predictive. After validation, we
99 performed global sensitivity and robustness analysis to estimate which parameters and
100 species controlled model performance. These analyses suggested complement was ro-
101 bust to any single therapeutic intervention. The only intervention that consistently reduced
102 C5a formation for all cases was a dual-knockdown of both C3 and C5. Taken together,
103 we developed a reduced order complement model that was computationally inexpensive,
104 and could easily be incorporated into pre-existing or new pharmacokinetic models of im-

¹⁰⁵ immune system function. The model described experimental data, and predicted the need
¹⁰⁶ for multiple points of intervention to disrupt complement activation.

107 **Results**

108 **Reduced order complement network.** The complement model described the alternate
109 and lectin pathways (Fig. 1). A trigger event initiated the lectin pathway, which activated
110 the cleavage of C2 and C4 into C2a, C2b, C4a and C4b respectively. Classical Pathway
111 (CP) C3 convertase (C4aC2b) then catalyzed the cleavage of C3 into C3a and C3b. The
112 alternate pathway was initiated through the spontaneous hydrolysis of C3 into C3a and
113 C3b (not C3w). The C3b fragment generated by hydrolysis (or by CP C3 convertase)
114 could then form the alternate pathway (AP) C3 convertase (C3bBb). We did not consider
115 C3w, nor the formation of the initial alternate C3 convertase (C3wBb). Rather, we as-
116 sumed C3w was equivalent to C3b and only modeled the formation of the main AP C3
117 convertase. Both the CP and AP C3 convertases catalyzed the cleavage of C3 into C3a
118 and C3b. A second C3b fragment could then bind with either the CP or AP C3 convertase
119 to form the CP or AP C5 convertase (C4bC2aC3b or C3bBbC3b). Both C5 convertases
120 catalyzed the cleavage of C5 into the C5a and C5b fragments. In this initial study, we
121 simplified the model by assuming both Factor B and Factor D were in excess. However,
122 we did explicitly account for two control proteins, Factor H and C4BP. Lastly, we did not
123 consider MAC formation, instead we stopped at C5a and C5b. Lectin pathway activation,
124 and C3/C5 convertase activity was modeled using a combination of saturation kinetics
125 and non-linear transfer functions, which facilitated a significant reduction in the size of the
126 model while maintaining performance. Binding interactions were modeled using mass-
127 action kinetics, where we assumed all binding was irreversible. Thus, while the reduced
128 order complement model encoded significant biology, it was highly compact consisting of
129 only 18 differential equations and 28 model parameters. Next, we estimated an ensemble
130 of model parameters from time series measurements of the C3a and C5a complement
131 proteins.

132 **Estimating an ensemble of reduced order complement models.** A critical challenge
133 for the development of any dynamic model is the estimation of model parameters. We
134 estimated an ensemble of complement model parameters in a hierarchical fashion using
135 *in vitro* time-series data sets generated with and without zymosan, a lectin pathway acti-
136 vator (20). The residual between model simulations and experimental measurements was
137 minimized using the dynamic optimization with particle swarms (DOPS) routine, starting
138 from an initial random parameter guess. Unless otherwise specified, all initial conditions
139 were assumed to be their mean physiological values. A hierarchical approach was taken
140 in which the alternate pathway parameters were estimated first and then fixed during the
141 estimation of the lectin pathway parameters. While we had significant training data, the
142 parameter estimation problem was underdetermined (we were not able to uniquely deter-
143 mine model parameters). Thus, instead of using a best-fit yet uncertain parameter set, we
144 estimated an ensemble of probable parameter sets ($N = 50$, see materials and methods).
145 The reduced order complement model ensemble captured the behavior of both the alter-
146 native and lectin pathways (Fig. 2). For the alternative pathway, we used C3a and C5a
147 measurements in the absence of zymosan, and only allowed the alternative parameters
148 to vary (Fig. 2A and B). On the other hand, lectin pathway parameters were estimated
149 from C3a and C5a measurements in the presence of 1g zymosan with alternate pathway
150 parameters fixed (Fig. 2C and D). The reduced order model reproduced a panel of alter-
151 nate and lectin pathway data sets in the neighborhood of physiological factor and inhibitor
152 concentrations. However, it was unclear whether the reduced order model could predict
153 new data, without updating the model parameters. To address this question, we fixed the
154 model parameters and simulated data sets not used for model training.

155 We tested the predictive power of the reduced order complement model with data
156 not used during model training (Fig. 3). Six validation cases were considered, three for
157 C3a and C5a, respectively. All model parameters and initial conditions were fixed for the

validation simulations (with the exception of zymosan). The ensemble of reduced order models predicted the qualitative dynamics of C3a formation (Fig. 3, left column), and C5a formation (Fig. 3, right column) at three inducer concentrations. However, there were shortcomings with model performance, especially for the C3a prediction. First, while the overall C3a trend was captured, the level of C3a was consistently under-predicted (outside of our 99% confidence interval) in all cases (Fig. 3, left column). We believe the C3a under-prediction was related to our choice of training data, and how we modeled C4BP interactions. We trained the model using 1g zymosan, but predicted cases with much less initiator. Next, the C4BP interactions were modeled as irreversible binding steps resulting in completely inactive complexes. However, the binding of C4BP with complement proteins is likely reversible, and CP C3 convertase may have residual activity even in the bound form. Thus, the model likely over-predicted the influence of C4BP. Second, while the C5a measurements were within the 99% confidence estimate, we failed to capture the concave down curvature for the 0.001g and 0.01g zymosan cases. The decreasing slope of the C5a may indicate cofactor limitation, or missing biology which we have not accounted for in the reduced order approach. Despite these shortcomings, we qualitatively predicted unseen experimental data, including correctly capturing the dynamic time scale of C3a formation, and the correct order of magnitude for the concentration of C5a for three inducer levels. Next, we used global sensitivity and robustness analysis to determine which parameters and species controlled the performance of the complement model.

Global analysis of the reduced order complement model. We conducted sensitivity analysis to estimate which parameters controlled the performance of the reduced order complement model. We calculated the sensitivity of the C3a and C5a residuals to changes in model parameters with and without zymosan for the ensemble of parameter sets (Fig. 4A - D). In the absence of zymosan (where only the alternative pathway is

active), $k_{f,C3b}$ (tickover formation of C3b) and $k_{d,C3a}$ (rate constant governing C3a degradation) controlled the C3a fit (Fig. 4A). Interestingly, $k_{c,C3}$ (the rate constant governing AP C3-convertase activity) was not sensitive in the absence of zymosan. Thus, C3a formation in the alternative pathway was more heavily influenced by the spontaneous hydrolysis of C3, rather than AP C3-convertase activity, in the absence of zymosan. On the other hand, the C5a residual was sensitive to tickover parameters e.g., $k_{f,C3b}$, and $k_{f,C3}$ (the rate constant governing AP C3 convertase formation) as well as parameters controlling AP C5 convertase activity in the absence of zymosan (Fig. 4B). Thus, the AP C3-convertase did not strongly influence C3a dynamics, but did effect C5a formation in the absence of zymosan. In the presence of zymosan, the C3a residual was controlled by the formation and activity of the CP C3 convertase, as well as tickover and degradation parameters (Fig. 4C). Further, the C5a residual was influenced by lectin initiation parameters, the formation and activity of CP C5 convertase, and the inhibition by C4BP in the presence of zymosan (Fig. 4D). Globally, sensitivity analysis suggested that lectin pathway parameters dominated system performance in the presence of zymosan, and that C5a formation was sensitive to both C3 and C5 convertase activity. In the absence of zymosan, the tickover parameters were important to both C3a and C5a formation, but C5a was also sensitive to C3 and C5 convertase activity. However, sensitivity coefficients are a local measure of how small changes in a parameter value effects model performance. To more closely simulate a clinical intervention e.g., administration of an anti-complement antibody, we performed robustness analysis. Robustness coefficients quantify the response of a marker to a macroscopic structural or operational perturbation to the network architecture. In this case, we computed how the C3a and C5a trajectories responded to a decrease in the initial abundance of C3 and/or C5.

Robustness analysis suggested there was no single intervention that inhibited complement activation in the presence of both initiation pathways (Fig. 5). We calculated robust-

ness indices for C3a and C5a for the parameter ensemble ($N = 50$) with and without the lectin pathway initiator. We simulated the addition of different doses of anti-complement antibody cocktails by decreasing the initial concentration of C3 or C5 or the combination of C3 and C5 by 50% and 90%. A \log_{10} transformed robustness index of zero indicated no effect due to the perturbation, whereas an index of less than zero indicated decreased C3a or C5a. As expected, a C5 knockdown had no effect on C3a formation for either the alternate (Fig. 5A, lanes 1 or 3) or lectin pathways (Fig. 5B, lanes 1 or 3). However, C3a abundance and to a lesser extent C5a abundance decreased with decreasing C3 concentration in the alternate pathway (Fig. 5A or B, lanes 1 or 2). This agreed with the sensitivity results; changes in AP C3-convertase formation or activity affected the downstream dynamics of C5a formation. Thus, these results suggested that C3 alone would be a reasonable target, especially given that C5a formation was surprisingly robust to C5 levels in the alternate pathway (Fig. 5A or B, lane 2). Yet, in lectin initiated complement activation, C5a levels were robust to the initial C3 concentration (Fig. 5A or B, lane 4). Thus, above some limiting threshold, even small concentrations of C3 and C5 convertases catalyzed the downstream formation of C5a. The only reliable intervention that consistently reduced C5a formation for all cases was a dual-knockdown. For example, a 90% decrease of both C3 and C5 reduced the formation of C5a by over an order of magnitude (Fig. 5B, lane 4).

229 **Discussion**

230 In this study, we developed an ensemble of experimentally validated reduced order com-
231 plement models. The modeling approach combined ordinary differential equations with
232 logical rules to produce a complement model with a limited number of equations and pa-
233 rameters. The reduced order model, which described the lectin and alternative pathways,
234 consisted of 18 differential equations with 28 parameters. Thus, the model was an order
235 of magnitude smaller and included more pathways than comparable mathematical mod-
236 els in the literature. We estimated an ensemble of model parameters from *in vitro* time
237 series measurements of the C3a and C5a complement proteins. Subsequently, we val-
238 idated the model on unseen C3a and C5a measurements that were not used for model
239 training. Despite its small size, the model was surprisingly predictive. After validation, we
240 performed global sensitivity and robustness analysis to estimate which parameters and
241 species controlled model performance. These analyses suggested complement was ro-
242 bust to any single therapeutic intervention. The only intervention that consistently reduced
243 C5a formation for all cases was a dual-knockdown of both C3 and C5. Taken together,
244 we developed a reduced order complement model that was computationally inexpensive,
245 and could easily be incorporated into pre-existing or new pharmacokinetic models of im-
246 mune system function. The model described experimental data, and predicted the need
247 for multiple points of intervention to disrupt complement activation.

248 Despite its importance, there has been a paucity of validated mathematical models
249 of complement pathway activation. To our knowledge, this study is one of the first com-
250 plement models that combined multiple initiation pathways with experimental validation
251 of important complement products like C5a. However, there have been several theoreti-
252 cal models of components of the cascade in the literature. Liu and co-workers modeled
253 the formation of C3a through the classical pathway using 45 non-linear ODEs (19). In
254 contrast, in this study we modeled lectin mediated C3a formation using only five ODEs.

Though we did not model all the initiation interactions in detail, especially the cross-talk between the lectin and classical pathways, we successfully captured C3a dynamics with respect to different concentrations of lectin initiators. The model also captured the dynamics of C3a and C5a formed from the alternate pathway using only seven ODEs. The reduced order model predictions of C5a were qualitatively similar to the theoretical complement model of Zewde et al which involved over 100 ODEs (16). However, we found that the quantity of C3a produced in the alternate pathway was nearly 1000 times the quantity of C5a produced. Though this was in agreement with the experimental data (20), it differed from the theoretical predictions made by Zewde et al. who showed C3a was 10^8 times the C5a concentration (16). In our model, the time profile of C5a generation from the lectin pathway changed with respect to the quantity of zymosan (the lectin pathway initiator). The lag phase for generation was inversely proportional to the initiator concentration. Korotaevskiy et al. showed a similar trend using a theoretical model of complement, albeit for much shorter time scales (18). Thus, the reduced order complement model performed similarly to existing large mechanistic models, despite being significantly smaller.

Global analysis of the complement model estimated potential important therapeutic targets. Complement malfunctions are implicated in a number of diseases, however the development of complement specific therapeutics has been challenging (3, 21). Previously, we have shown that mathematical modeling and sensitivity analysis can be useful tools to estimate therapeutically important mechanisms in biochemical networks (22–25). In this study, we analyzed a validated ensemble of reduced order complement models to estimate therapeutically important mechanisms. In presence of an initiator, C5a formation was primarily sensitive to the lectin initiation parameters, and parameters governing the conversion of C5 to C5a and C5b. This result agrees well with the current protease inhibitors targeting initiating complexes, including mannose-associated serine proteases 1 and 2 (MASP-1,2) (26). The most commonly used anti-complement drug eculizumab

281 (21), targets the C5 protein which is cleaved to form C5a. Our sensitivity analysis showed
282 that kinetic parameters governing C5 conversion were sensitive in both lectin initiated and
283 alternate pathways, thus agreeing with targeting C5 protein. The formation of basal C3b
284 was also a sensitive parameter in the formation of C3a through the alternate pathway.
285 Thus, this mechanism can act as a target for both C3a and C5a inhibitors. Lectin initiated
286 C3a formation showed a number of sensitive parameters. This included the lectin initi-
287 ation parameters that controlled C5a formation, C3 convertase inhibition by C4BP, and
288 parameters governing C3 convertase activity. All these mechanisms are potential drug
289 targets.

290 To further validate these results from sensitivity analysis about potential drug targets
291 we did a robustness analysis. We knocked down C3 and C5 levels and studied their im-
292 pact on the generation of C3a and C5a. The C3a and C5a levels in the lectin pathway
293 were strongly influenced by initial levels of C3 and C5. Thus direct inhibition of C3 and
294 C5, or targeting complexes (MASP complex, C3 and C5 convertases) that act on C3 and
295 C5 have a direct impact on production of C3a and C5a. This is also in agreement with
296 sensitivity analysis that C5 is a good drug target. A number of drugs targeting C5 are
297 being developed. For example LFG316 by Novartis is being used to target C5 in cases
298 of Age-Related Macular Degeneration (27), Mubodina is an antibody that targets C5 in
299 the treatment of Atypical Hemolytic-Uremic Syndrome (aHUS) (28), Coversin is a small
300 molecule targeting C5 (29), Zimura is an aptamer targeting C5 (30), small peptides and
301 RNAi are also being used to inhibit C5 (31). Another important conclusion that can be
302 drawn together from sensitivity and robustness analysis is that C3 and C5 convertases
303 can be important therapeutic targets. Though knockdown of C3 and C5 affects C3a and
304 C5a levels downstream, the abundance and turnover rate (32, 33) of these proteins make
305 them difficult targets. Thus targeting C3 and C5 directly will require high dosage of drugs.
306 It is also well known that eculizumab dosage needs to be adjusted while treating for Atyp-

307 ical Hemolytic-Uremic Syndrome (aHUS), a disease that is caused due to uncontrolled
308 complement activation (34). The issue of high dosage can potentially be circumvented
309 by targeting convertases or fragile mechanisms that involve C3, C5 or their activated
310 components. Our analysis shows that formation and assembly of these convertases are
311 sensitive mechanisms that strongly impact downstream proteins like C5a. Formation of
312 convertases is inhibited by targeting upstream protease complexes like MASP-1,2 from
313 lectin pathway (or C1r, C1s from classical pathway). For example, Omeros is a protease
314 inhibitor that targets MASP-2 complex and thereby inhibits formation of downstream con-
315 vertases (35). Lampalizumab (an immunoglobulin) and Bikaciomab (an antibody frag-
316 ment) target Factor B and Factor D respectively. Factor B and Factor D are crucial to
317 formation alternate pathway convertases (36, 37). Novelmed Therapeutics recently de-
318 veloped antibody, NM9401 against propedin, a small protein that stabilizes alternate C3
319 convertase (38). Cobra Venom Factor (CVF), an analogue of C3b has been used to bind
320 to Factor B to regulate alternate convertases (39). Thus, analysis of the ensemble of com-
321 plement models identified potentially important therapeutic targets that are consistent with
322 therapeutic strategies that are under development.

323 The performance of the complement model was impressive given its limited size. How-
324 ever, there are several questions that should be explored further. A logical progression for
325 this work would be to expand the network to include the classical pathway and the forma-
326 tion of the membrane attack complex (MAC). However, it is unclear whether the addition
327 of the classical pathway will decrease the predictive quality of our existing model. Liu
328 et al have shown cross-talk between the activation of the classical and lectin pathways
329 that could influence model performance (19). One potential approach to address such
330 difficulties would be to incorporate C reactive proteins (CRP) and L-ficolin (LF) into the
331 model, both of which are involved with the initiation of classical and lectin pathways. Liu
332 et al. showed that under inflammation conditions interactions between lectin and classical

pathways was mediated through CRP and LF (19). Thus incorporating these two proteins would help us in modeling cross talk. Time course measurements of MAC abundance (and MAC formation dynamics) are also scarce, making the inclusion of MAC challenging. Next, we should address the under-prediction of C3a. We believe the C3a under-prediction can be attributed to how we modeled C4BP interactions. C4BP interactions were modeled as irreversible binding steps resulting in completely inactive complexes; however, the binding of C4BP with complement proteins is likely reversible and C4BP-bound convertases may have residual activity. We also did not capture the maximum concentration of C3a at low initiator levels. One possible reason for this could be the C2-by-pass pathway, which was not included in the model. This pathway further accelerates C3a production without the involvement of a C3 convertase. Currently the C3a in the model is generated only through the activity of a C3 convertase. Incorporating this additional step within the reduced order modeling framework would be a future direction that we need to consider. We should test alternative model structures which include reversible C4BP binding, and partially active convertases. Alternatively, we could also perform sensitivity analysis on the C3a prediction residual to determine which parameters controlled the C3a prediction.

350 **Materials and Methods**

351 **Formulation and solution of the complement model equations.** We used ordinary
 352 differential equations (ODEs) to model the time evolution of complement proteins (x_i) in
 353 the reduced order model:

$$\frac{dx_i}{dt} = \sum_{j=1}^{\mathcal{R}} \sigma_{ij} r_j(\mathbf{x}, \epsilon, \mathbf{k}) \quad i = 1, 2, \dots, \mathcal{M} \quad (1)$$

354 where \mathcal{R} denotes the number of reactions and \mathcal{M} denotes the number of protein species
 355 in the model. The quantity $r_j(\mathbf{x}, \epsilon, \mathbf{k})$ denotes the rate of reaction j . Typically, reaction j is
 356 a non-linear function of biochemical and enzyme species abundance, as well as unknown
 357 model parameters \mathbf{k} ($\mathcal{K} \times 1$). The quantity σ_{ij} denotes the stoichiometric coefficient for
 358 species i in reaction j . If $\sigma_{ij} > 0$, species i is produced by reaction j . Conversely, if $\sigma_{ij} < 0$,
 359 species i is consumed by reaction j , while $\sigma_{ij} = 0$ indicates species i is not connected
 360 with reaction j . Species balances were subject to the initial conditions $\mathbf{x}(t_0) = \mathbf{x}_0$.

361 Rate processes were written as the product of a kinetic term (\bar{r}_j) and a control term
 362 (v_j) in the complement model. The kinetic term for the formation of C4a, C4b, C2a and
 363 C2b, lectin pathway activation, and C3 and C5 convertase activity was given by:

$$\bar{r}_j = k_j^{max} \epsilon_i \left(\frac{x_s^\eta}{K_{js}^\eta + x_s^\eta} \right) \quad (2)$$

364 where k_j^{max} denotes the maximum rate for reaction j , ϵ_i denotes the abundance of the
 365 enzyme catalyzing reaction j , η denotes a cooperativity parameter, and K_{js} denotes the
 366 saturation constant for species s in reaction j . We used mass action kinetics to model
 367 protein-protein binding interactions within the network:

$$\bar{r}_j = k_j^{max} \prod_{s \in m_j^-} x_s^{-\sigma_{sj}} \quad (3)$$

368 where k_j^{max} denotes the maximum rate for reaction j , σ_{sj} denotes the stoichiometric co-
 369 efficient for species s in reaction j , and $s \in m_j$ denotes the set of *reactants* for reaction
 370 j . We assumed all binding interactions were irreversible. The control terms $0 \leq v_j \leq 1$
 371 depended upon the combination of factors which influenced rate process j . For each rate,
 372 we used a rule-based approach to select from competing control factors. If rate j was in-
 373 fluenced by $1, \dots, m$ factors, we modeled this relationship as $v_j = \mathcal{I}_j(f_{1j}(\cdot), \dots, f_{mj}(\cdot))$
 374 where $0 \leq f_{ij}(\cdot) \leq 1$ denotes a regulatory transfer function quantifying the influence of
 375 factor i on rate j . The function $\mathcal{I}_j(\cdot)$ is an integration rule which maps the output of regu-
 376 latory transfer functions into a control variable. Each regulatory transfer function took the
 377 form:

$$f_{ij}(\mathcal{Z}_i, k_{ij}, \eta_{ij}) = k_{ij}^{\eta_{ij}} \mathcal{Z}_i^{\eta_{ij}} / (1 + k_{ij}^{\eta_{ij}} \mathcal{Z}_i^{\eta_{ij}}) \quad (4)$$

378 where \mathcal{Z}_i denotes the abundance of factor i , k_{ij} denotes a gain parameter, and η_{ij} denotes
 379 a cooperativity parameter. In this study, we used $\mathcal{I}_j \in \{min, max\}$ (40). If a process has
 380 no modifying factors, $v_j = 1$. The model equations were implemented in MATLAB and
 381 solved using the ODE23s routine (The Mathworks, Natick MA). The complement model
 382 code and parameter ensemble is freely available under an MIT software license and can
 383 be downloaded from <http://www.varnerlab.org>.

384 **Estimation of an ensemble of complement model parameters.** We minimized the
 385 residual between simulations and experimental C3a and C5a measurements using Dy-
 386 namic Optimization with Particle Swarms (DOPS). DOPS minimized the objective:

$$\min_{\mathbf{k}} \sum_{\tau=1}^{\mathcal{T}} \sum_{j=1}^S \left(\frac{\hat{x}_j(\tau) - x_j(\tau, \mathbf{k})}{\omega_j(\tau)} \right)^2 \quad (5)$$

387 where $\hat{x}_j(\tau)$ denotes the measured value of species j at time τ , $x_j(\tau, \mathbf{k})$ denotes the sim-
 388 ulated value for species j at time τ , and $\omega_j(\tau)$ denotes the experimental measurement

variance for species j at time τ . The outer summation is with respect to time, while the inner summation is with respect to state. DOPS is a novel metaheuristic that combines multi swarm particle swarm optimization (PSO) with a greedy global optimization algorithm called dynamically dimensioned search (DDS). DOPS is faster than conventional global optimizers and has the ability to find near optimal solutions for high dimensional systems within a relatively few function evaluations. It uses an adaptive switching strategy based on error convergence rates to switch from the particle swarm to DDS search phases. This enables DOPS to quickly estimate globally optimal or near optimal solutions even in the presence of many local minima. In the swarm search, for each iteration the particles compute error within each sub-swarm by evaluating the model equations using their specific parameter vector realization. From each of these points within a sub-swarm a local best is identified. This along with the particle best within the sub-swarm S_k is used to update the parameter estimate for each particle using the following rules:

$$z_{i,j} = \theta_1 z_{i,j-1} + \theta_2 r_1 (\mathcal{L}_i - z_{i,j-1}) + \theta_3 r_2 (\mathcal{G}_k - z_{i,j-1}) \quad (6)$$

where $z_{i,j}$ is the parameter vector, $(\theta_1, \theta_2, \theta_3)$ were adjustable parameters, \mathcal{L}_i denotes the best solution found by particle i within sub-swarm S_k for function evaluations $1 \rightarrow j-1$, and \mathcal{G}_k denotes the best solution found over all particles within sub-swarm S_k . The quantities r_1 and r_2 denote uniform random vectors with the same dimension as the number of unknown model parameters ($K \times 1$). At the conclusion of the swarm phase, the overall best particle, \mathcal{G}_k , over the k sub-swarms was used to initialize the DDS phase. For the DDS phase, the best parameter estimate was updated using the rule:

$$\mathcal{G}_{new}(J) = \begin{cases} \mathcal{G}(J) + \mathbf{r}_{normal}(J)\sigma(J), & \text{if } \mathcal{G}_{new}(J) < \mathcal{G}(J). \\ \mathcal{G}(J), & \text{otherwise.} \end{cases} \quad (7)$$

409 where \mathbf{J} is a vector representing the subset of dimensions that are being perturbed, \mathbf{r}_{normal}
410 denotes a normal random vector of the same dimensions as \mathcal{G} , and σ denotes the pertur-
411 bation amplitude:

$$\sigma = R(\mathbf{p}^U - \mathbf{p}^L) \quad (8)$$

412 where R is the scalar perturbation size parameter, \mathbf{p}^U and \mathbf{p}^L are $(\mathcal{K} \times 1)$ vectors that
413 represent the maximum and minimum bounds on each dimension. The set \mathbf{J} was con-
414 structed using a monotonically decreasing probability function \mathcal{P}_i that represents a thresh-
415 old for determining whether a specific dimension j was perturbed or not. DDS updates
416 are greedy; \mathcal{G}_{new} becomes the new solution vector only if it is better than \mathcal{G} . At the end
417 of DDS phase we obtain the optimal vector \mathcal{G} which we use for plotting best fits against
418 the experimental data, and for generating a parameter ensemble. The DOPS routine
419 was implemented in MATLAB (The Mathworks, Natick MA) and can be downloaded from
420 <http://www.varnerlab.org> under an MIT software license.

421 An ensemble of parameters was obtained by randomly perturbing the optimal parame-
422 ter set within bounds established by analyzing the results of repeated DOPS runs. There-
423 after, the optimal parameter vector was perturbed within these bounds for approximately
424 100,000 iterations. Within each iteration the quality of perturbed vector was measured
425 using goodness of fit (model residual). If the residual was too high or the perturbed vector
426 generated a numerical error, the vector was rejected, otherwise it was accepted. We se-
427 lected an ensemble of $N = 50$ parameter sets for this study using this sampling procedure.
428 The best fit parameter set, and parameter ensemble is available in tab-delimited plain-text
429 format from the Complement model GitHub repository.

430 **Sensitivity and robustness analysis of complement model performance.** We con-
431 ducted global sensitivity and robustness analysis to estimate which parameters and species
432 controlled the performance of the reduced order model. We computed the total variance-

433 based sensitivity index of each parameter relative to the training residual for the C3a
 434 alternate, C5a alternate, C3a lectin, and C5a lectin cases using the Sobol method (41).
 435 The sampling bounds for each parameter were established from the minimum and maxi-
 436 mum value for that parameter in the parameter ensemble. We used the sampling method
 437 of Saltelli *et al.* to compute a family of $N(2d + 2)$ parameter sets which obeyed our pa-
 438 rameter ranges, where N was the number of trials per parameters, and d was the number
 439 of parameters in the model (42). In our case, $N = 200$ and $d = 28$, so the total sensitivity
 440 indices were computed using 11,600 model evaluations. The variance-based sensitivity
 441 analysis was conducted using the SALib module encoded in the Python programming
 442 language (43).

443 Robustness coefficients quantify the response of a marker to a structural or operational
 444 perturbation to the network architecture. Robustness coefficients were calculated as
 445 shown previously (44). Log-transformed robustness coefficients denoted by $\hat{\alpha}(i, j, t_o, t_f)$
 446 are defined as:

$$\hat{\alpha}(i, j, t_o, t_f) = \log_{10} \left[\left(\int_{t_o}^{t_f} x_i(t) dt \right)^{-1} \left(\int_{t_o}^{t_f} x_i^{(j)}(t) dt \right) \right] \quad (9)$$

447 Here t_o and t_f denote the initial and final simulation time, while i and j denote the indices
 448 for the marker and the perturbation, respectively. A value of $\hat{\alpha}(i, j, t_o, t_f) > 0$, indicates
 449 increased marker abundance, while $\hat{\alpha}(i, j, t_o, t_f) < 0$ indicates decreased marker abun-
 450 dance following perturbation j . If $\hat{\alpha}(i, j, t_o, t_f) \sim 0$, perturbation j did not influence the
 451 abundance of marker i . In this study, we perturbed the initial condition of C3 or C5 or
 452 a combination of C3 and C5 by 50% or 90% and measured the area under the curve
 453 (AUC) of C3a or C5a with and without lectin initiator. Log-transformed robustness coeffi-
 454 cients were calculated for every member of the ensemble, where the mean $\pm 1 \times$ standard-
 455 deviation are reported.

456 **Competing interests**

457 The authors declare that they have no competing interests.

458 **Author's contributions**

459 J.V directed the study. A.S developed the reduced order complement model and the
460 parameter ensemble. A.S, W.D and M.M analyzed the model ensemble, and generated
461 figures for the manuscript. The manuscript was prepared and edited for publication by
462 A.S, W.D, M.M and J.V.

463 **Acknowledgements**

464 We gratefully acknowledge the suggestions from the anonymous reviewers to improve
465 this manuscript.

466 **Funding**

467 This study was supported by an award from the US Army and Systems Biology of Trauma
468 Induced Coagulopathy (W911NF-10-1-0376) to J.V. for the support of A.S.

469 **References**

- 470 1. Nuttall G (1888) Experimente über die bacterienfeindlichen Einflüsse des thierischen
471 Körpers. Z Hyg Infektionskr 4: 353-394.
- 472 2. Ricklin D, Hajishengallis G, Yang K, Lambris JD (2010) Complement: a key system
473 for immune surveillance and homeostasis. NAT IMMUNOL 11: 785–797.
- 474 3. Ricklin D, Lambris JD (2007) Complement-targeted therapeutics. NAT BIOTECHNOL
475 25: 1265-1275.
- 476 4. Rittirsch D, Flierl MA, Ward PA (2008) Harmful molecular mechanisms in sepsis. NAT
477 REV IMMUNOL 8: 776–787.
- 478 5. Sarma JV, Ward PA (2011) The complement system. Cell Tissue Res 343: 227–235.
- 479 6. Ricklin D, Lambris JD (2013) Complement in immune and inflammatory disorders:
480 pathophysiological mechanisms. J Immunol 190: 3831–3838.
- 481 7. Walport MJ (2001) Complement. first of two parts. N Engl J Med 344: 1058-66.
- 482 8. Walport MJ (2001) Complement. second of two parts. N Engl J Med 344: 1140-4.
- 483 9. Pangburn MK, Müller-Eberhard HJ (1984) The alternative pathway of complement.
484 Semin Immunopathol .
- 485 10. Walker D, Yasuhara O, Patston P, McGeer E, McGeer P (1995) Complement c1 in-
486 hibitor is produced by brain tissue and is cleaved in alzheimer disease. Brain Res
487 675: 75–82.
- 488 11. Blom AM, Kask L, Dahlbäck B (2001) Structural requirements for the complement
489 regulatory activities of c4bp. J Biol Chem 276: 27136–27144.
- 490 12. Riley-Vargas RC, Gill DB, Kemper C, Liszewski MK, Atkinson JP (2004) Cd46: ex-
491 panding beyond complement regulation. Trends Immunol 25: 496–503.
- 492 13. Lukacik P, Roversi P, White J, Esser D, Smith G, et al. (2004) Complement regulation
493 at the molecular level: the structure of decay-accelerating factor. Proc Natl Acad Sci
494 USA 101: 1279–1284.

- 495 14. Liszewski MK, Farries TC, Lublin DM, Rooney IA, Atkinson JP (1995) Control of the
496 complement system. *Adv Immunol* 61: 201–283.
- 497 15. Chauhan A, Moore T (2006) Presence of plasma complement regulatory proteins
498 clusterin (apo j) and vitronectin (s40) on circulating immune complexes (cic). *Clin
499 Exp Immunol* 145: 398–406.
- 500 16. Zewde N, Gorham Jr RD, Dorado A, Morikis D (2016) Quantitative modeling of the
501 alternative pathway of the complement system. *PLoS one* 11: e0152337.
- 502 17. Hirayama H, Yoshii K, Ojima H, Kawai N, Gotoh S, et al. (1996) Linear systems analy-
503 sis of activating processes of complement system as a defense mechanism. *Biosys-
504 tems* 39: 173–185.
- 505 18. Korotaevskiy AA, Hanin LG, Khanin MA (2009) Non-linear dynamics of the comple-
506 ment system activation. *Math Biosci* 222: 127–143.
- 507 19. Liu B, Zhang J, Tan PY, Hsu D, Blom AM, et al. (2011) A computational and experi-
508 mental study of the regulatory mechanisms of the complement system. *PLoS Comput
509 Biol* 7: e1001059.
- 510 20. Morad HO, Belete SC, Read T, Shaw AM (2015) Time-course analysis of c3a and
511 c5a quantifies the coupling between the upper and terminal complement pathways in
512 vitro. *J Immunol Methods* 427: 13–18.
- 513 21. Morgan BP, Harris CL (2015) Complement, a target for therapy in inflammatory and
514 degenerative diseases. *NAT REV DRUG DISCOV* 14: 857-877.
- 515 22. Luan D, Zai M, Varner JD (2007) Computationally derived points of fragility of a human
516 cascade are consistent with current therapeutic strategies. *PLoS Comput Biol* 3:
517 e142.
- 518 23. Nayak S, Salim S, Luan D, Zai M, Varner JD (2008) A test of highly optimized tol-
519 erance reveals fragile cell-cycle mechanisms are molecular targets in clinical cancer
520 trials. *PLoS One* 3: e2016.

- 521 24. Tasseff R, Nayak S, Salim S, Kaushik P, Rizvi N, et al. (2010) Analysis of the molecular
522 networks in androgen dependent and independent prostate cancer revealed fragile
523 and robust subsystems. PLoS One 5: e8864.
- 524 25. Rice NT, Szlam F, Varner JD, Bernstein PS, Szlam AD, et al. (2016) Differential con-
525 tributions of intrinsic and extrinsic pathways to thrombin generation in adult, maternal
526 and cord plasma samples. PLoS One 11: e0154127.
- 527 26. Héja D, Harmat V, Fodor K, Wilmanns M, Dobó J, et al. (2012) Monospecific inhibitors
528 show that both mannan-binding lectin-associated serine protease-1 (masp-1) and-2
529 are essential for lectin pathway activation and reveal structural plasticity of masp-2. J
530 Biol Chem : 20290–20300.
- 531 27. Roguska M, Splawski I, Diefenbach-Streiber B, Dolan E, Etemad-Gilbertson B, et al.
532 (2014) Generation and characterization of Ifg316, a fully-human anti-c5 antibody for
533 the treatment of age-related macular degeneration. Investigative Ophthalmology &
534 Visual Science : 3433–3433.
- 535 28. Melis JP, Strumane K, Ruuls SR, Beurskens FJ, Schuurman J, et al. (2015) Com-
536 plement in therapy and disease: Regulating the complement system with antibody-
537 based therapeutics. Molecular immunology : 117–130.
- 538 29. Weston-Davies WH, Nunn MA, Pinto FO, Mackie IJ, Richards SJ, et al. (2014) Clin-
539 ical and immunological characterisation of coversin, a novel small protein inhibitor of
540 complement c5 with potential as a therapeutic agent in pnh and other complement
541 mediated disorders. Blood : 4280–4280.
- 542 30. Epstein D, Kurz JC (2007). Complement binding aptamers and anti-c5 agents useful
543 in the treatment of ocular disorders. US Patent App. 12/224,708.
- 544 31. Borodovsky A, Yucius K, Sprague A, Banda NK, Holers VM, et al. (2014) Aln-cc5, an
545 investigational rnai therapeutic targeting c5 for complement inhibition. Complement
546 20: 40.

- 547 32. Sissons J, Liebowitch J, Amos N, Peters D (1977) Metabolism of the fifth component
548 of complement, and its relation to metabolism of the third component, in patients with
549 complement activation. *J Clin Invest* 59: 704.
- 550 33. Swaak A, Hannema A, Vogelaar C, Boom F, van Es L, et al. (1982) Determination of
551 the half-life of c3 in patients and its relation to the presence of c3-breakdown products
552 and/or circulating immune complexes. *Rheumatol Int* : 161–166.
- 553 34. Noris M, Galbusera M, Gastoldi S, Macor P, Banterla F, et al. (2014) Dynamics of
554 complement activation in ahus and how to monitor eculizumab therapy. *Blood* : 1715–
555 1726.
- 556 35. Schwaeble HW, Stover CM, Tedford CE, Parent JB, Fujita T (2011). Methods for
557 treating conditions associated with masp-2 dependent complement activation. US
558 Patent 7,919,094.
- 559 36. Katschke KJ, Wu P, Ganesan R, Kelley RF, Mathieu MA, et al. (2012) Inhibiting al-
560 ternative pathway complement activation by targeting the factor d exosite. *Journal of*
561 *Biological Chemistry* : 12886–12892.
- 562 37. Hu X, Holers VM, Thurman JM, Schoeb TR, Ramos TN, et al. (2013) Therapeutic in-
563 hibition of the alternative complement pathway attenuates chronic eae. *Mol Immunol*
564 : 302–308.
- 565 38. Bansal R (2014). Humanized and chimeric anti-properdin antibodies. US Patent
566 8,664,362.
- 567 39. Vogel CW, Fritzinger DC, Hew BE, Thorne M, Bammert H (2004) Recombinant cobra
568 venom factor. *Molecular immunology* : 191–199.
- 569 40. Sagar A, Varner JD (2015) Dynamic modeling of the human coagulation cascade
570 using reduced order effective kinetic models. *Processes* 3: 178.
- 571 41. Sobol I (2001) Global sensitivity indices for nonlinear mathematical models and their
572 monte carlo estimates. *MATH COMPUT SIMULAT* 55: 271 - 280.

- 573 42. Saltelli A, Annoni P, Azzini I, Campolongo F, Ratto M, et al. (2010) Variance based
574 sensitivity analysis of model output. design and estimator for the total sensitivity index.
575 Comput Phys Commun 181: 259–270.
- 576 43. Herman J. Salib: Sensitivity analysis library in python (numpy). con-
577 tains sobol, morris, fractional factorial and fast methods. available online:
578 <https://github.com/jdherman/salib>.
- 579 44. Tasseff R, Nayak S, Song SO, Yen A, Varner JD (2011) Modeling and analysis
580 of retinoic acid induced differentiation of uncommitted precursor cells. Integr Biol
581 (Camb) 3: 578-91.

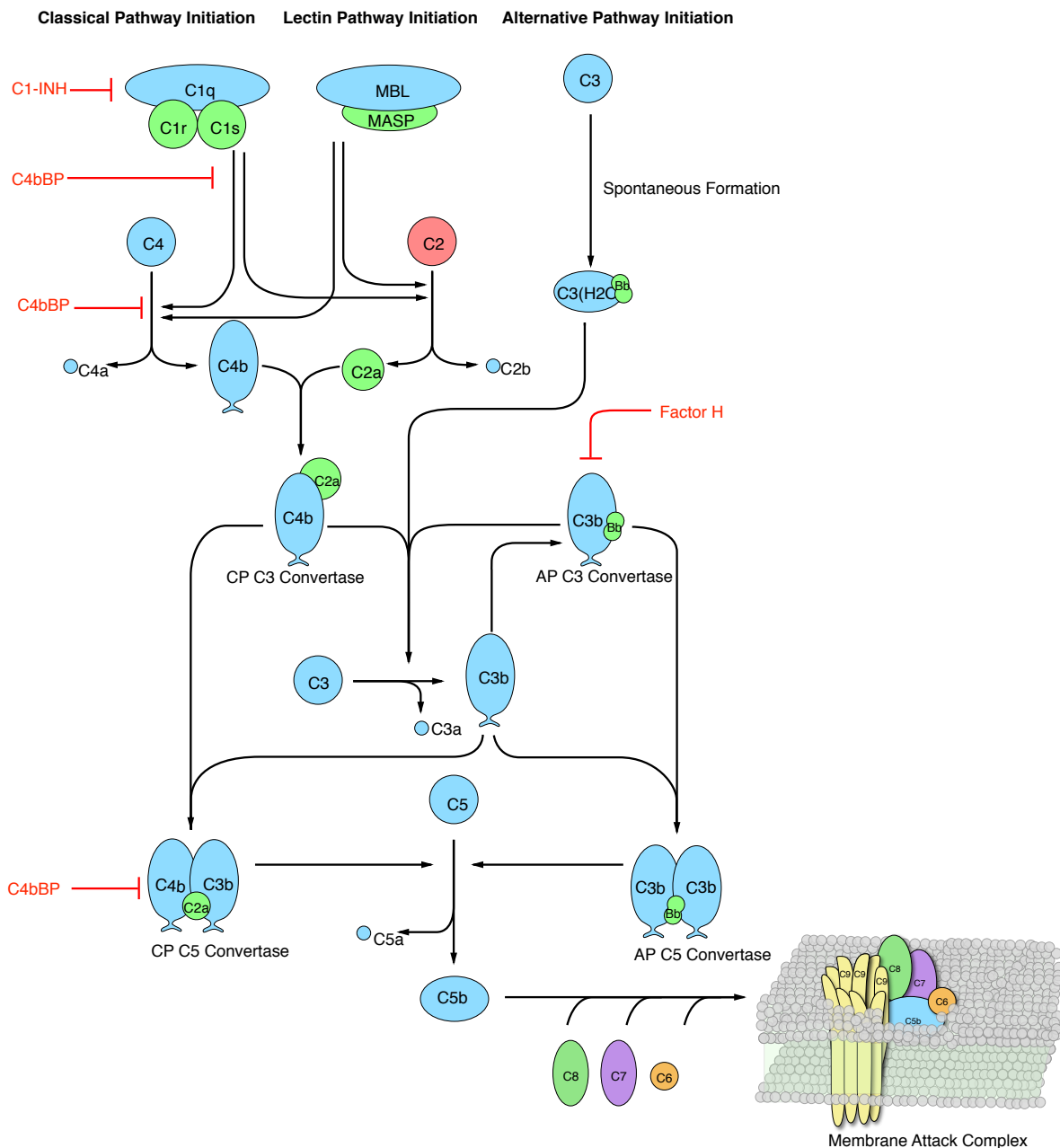


Fig. 1: Simplified schematic of the human complement system. The complement cascade is activated through three pathways: the classical, the lectin, and the alternate pathways. Complement initiation results in the formation of classical or alternative C3 convertases, which amplify the initial complement response and signal to the adaptive immune system by cleaving C3 into C3a and C3b. C3 convertases further react to form C5 convertases which catalyze the cleavage of the C5 complement protein to C5a and C5b. C5b is critical to the formation of the membrane attack complex (MAC), while C5a recruits an adaptive immune response.

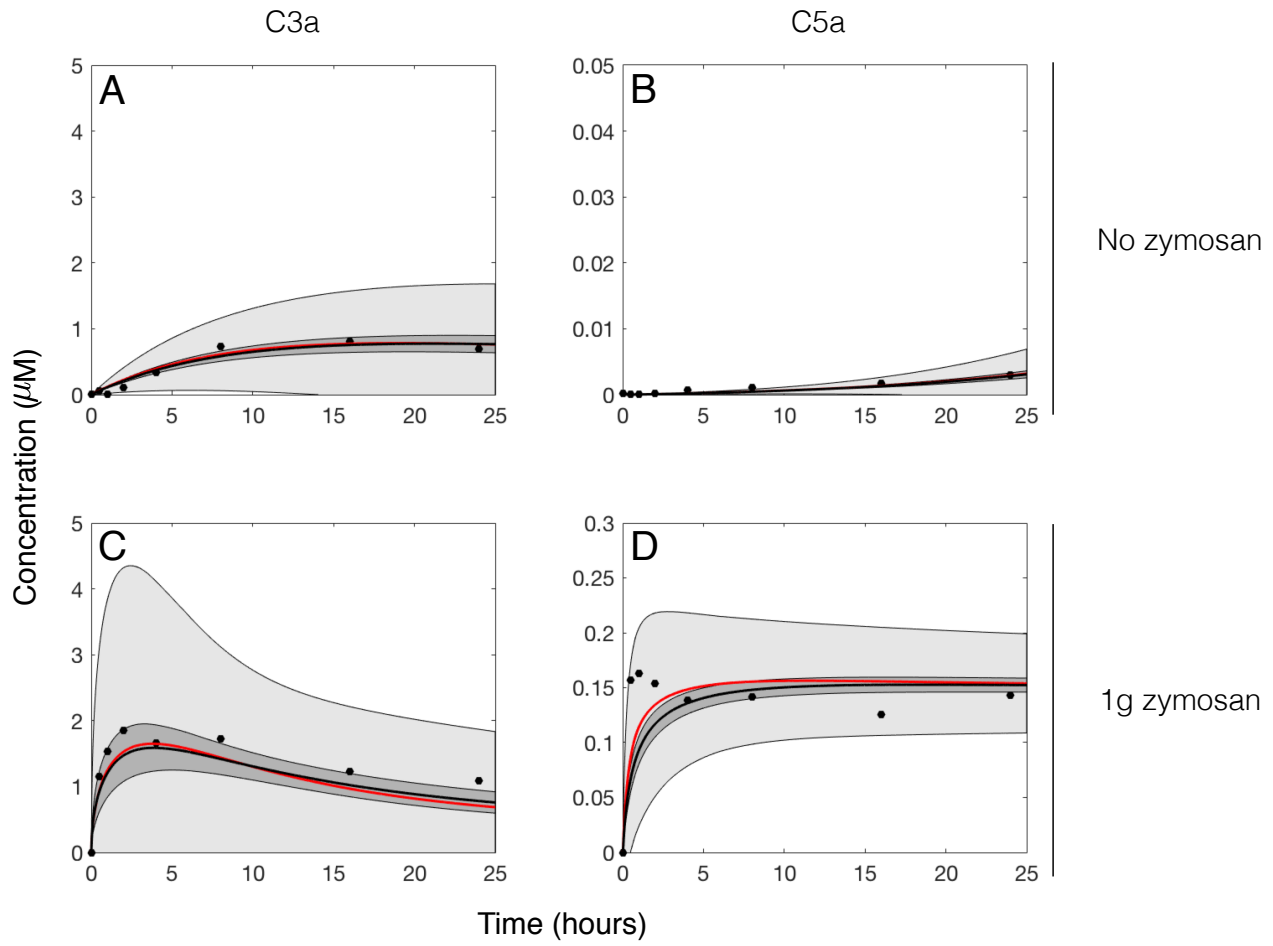


Fig. 2: Reduced order complement model training. Model parameters were estimated using Dynamic Optimization with Particle Swarms (DOPS) from C3a and C5a measurements with and without zymosan (20). The model was trained using C3a and C5a data generated from the alternative pathway (**A–B**) and lectin pathway initiated with 1g zymosan (**C–D**). The solid red line shows the simulation with the best-fit parameter set, the solid black lines show the simulated mean value of C3a or C5a for the ensemble ($N = 50$). The dark shaded region denotes the 99% confidence interval of the simulated mean concentrations, while the light shaded region denotes the 99% confidence interval of the best-fit simulation for C3a and C5a. All initial conditions were assumed to be at their physiological serum levels unless otherwise noted.

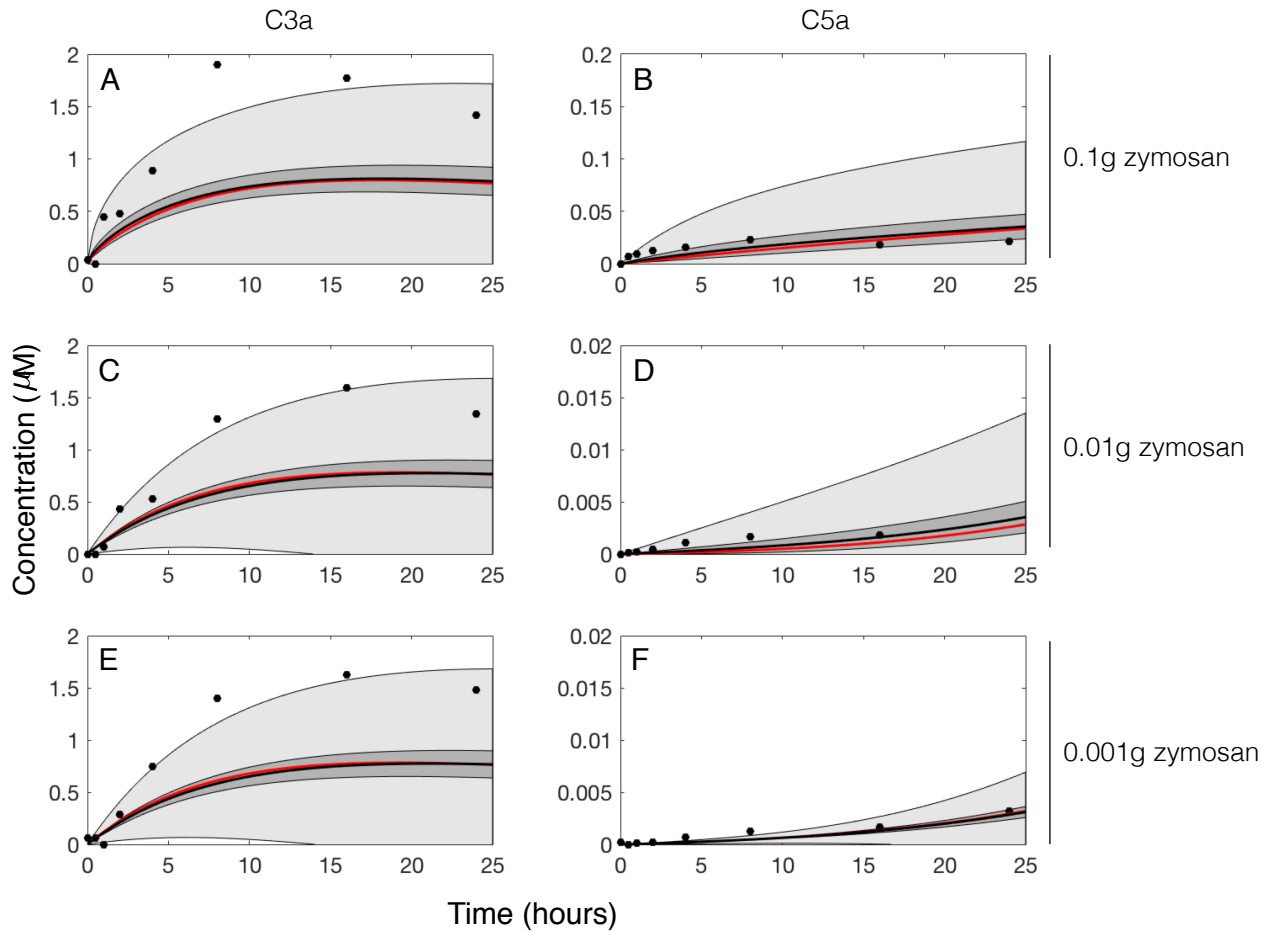


Fig. 3: Reduced order complement model predictions. The reduced order coagulation model parameter estimates were tested against data not used during model training (20). Simulations of C3a and C5a generated in the lectin pathway using 0.1g, 0.01g, and 0.001g zymosan were compared with the corresponding experimental measurement. The solid red line shows the simulation with the best-fit parameter set, the solid black lines show the simulated mean value of C3a or C5a for the ensemble ($N = 50$). The dark shaded region denotes the 99% confidence interval of the simulated mean concentrations, while the light shaded region denotes the 99% confidence interval of the best-fit simulation for C3a and C5a. All initial conditions were assumed to be at their physiological serum levels unless otherwise noted.

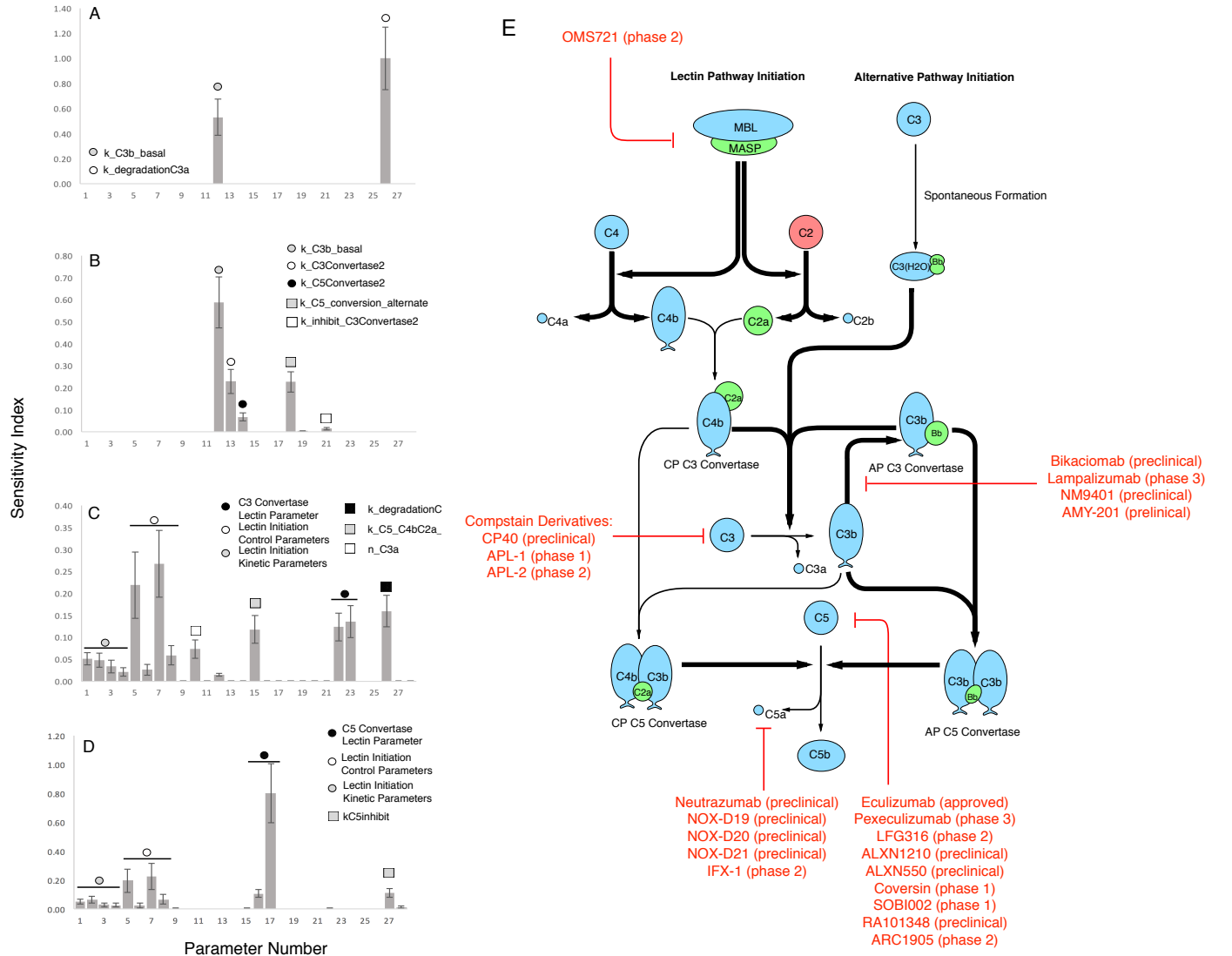
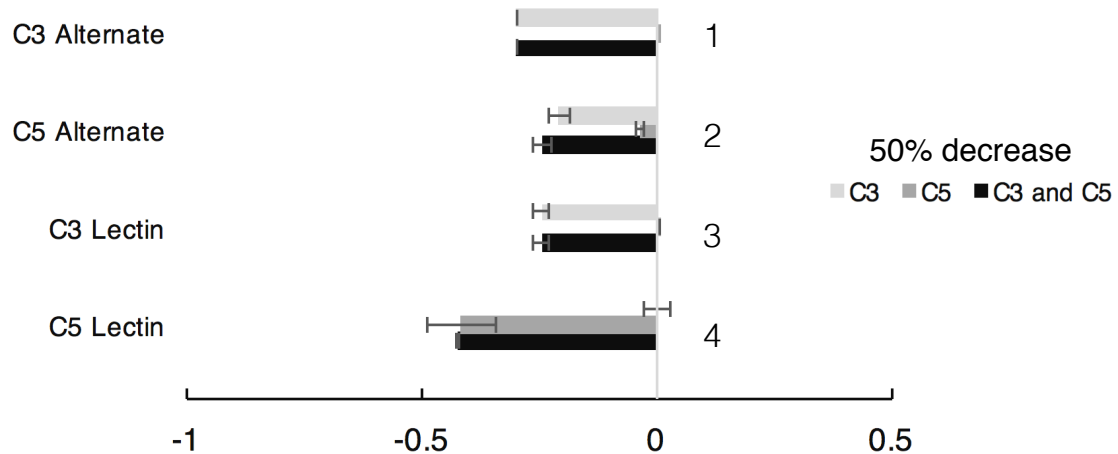


Fig. 4: Global sensitivity analysis of the reduced order complement model. Sensitivity analysis was conducted on the four cases used for model training. **A:** Sensitivity of the C3a residual at 0g zymosan, **B:** Sensitivity of the C5a residual at 0g zymosan, **C:** Sensitivity of the C3a residual at 1g zymosan, and **D:** Sensitivity of the C5a residual at 1g zymosan. The bars denote the mean total sensitivity index for each parameter, while the error bars denote the 95% confidence interval. **E:** Pathways controlled by the sensitivity parameters. Bold black lines indicates the pathway is governed by one or more sensitive parameters and the red lines shows some of the current therapeutics targets. Red indicates current complement therapeutics.

A



B

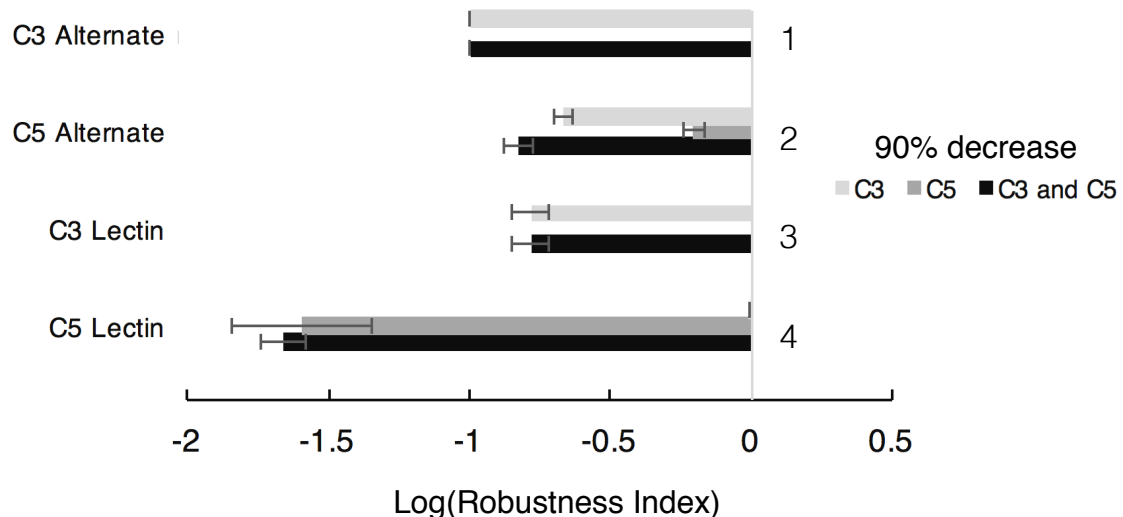


Fig. 5: Robustness analysis of the complement model with respect to C3 and C5 initial conditions. Robustness analysis was conducted on the four cases used for model training: C3a alternate (0g zymosan), C5a alternate (0g zymosan), C3a lectin (1g zymosan), and C5a lectin (1g zymosan), by reducing the initial concentration of C3 and/or C5 by **A** 50% and **B** 90 %. The bars denote the log-transformated robustness index while error bars denote one standard deviation. At zero, the perturbed initial concentration has no impact on the measured output. A log-transformed robustness index less than zero indicates a negative relation between the perturbed initial concentration and the measured output.

582 **Supplemental materials.**

583 **Model equations.** The reduced-order complement model consisted of 18 ordinary dif-
 584 ferential equations, 12 rate equations, and two control equations:

$$\frac{dx_1}{dt} = -r_1 f_1 \quad (\text{S1})$$

$$\frac{dx_2}{dt} = -r_2 f_2 \quad (\text{S2})$$

$$\frac{dx_3}{dt} = r_1 f_1 \quad (\text{S3})$$

$$\frac{dx_4}{dt} = r_1 f_1 - r_6 \quad (\text{S4})$$

$$\frac{dx_5}{dt} = r_2 f_2 - r_6 \quad (\text{S5})$$

$$\frac{dx_6}{dt} = r_2 f_2 \quad (\text{S6})$$

$$\frac{dx_7}{dt} = r_3 - r_4 - r_5 \quad (\text{S7})$$

$$\frac{dx_8}{dt} = r_3 + r_4 + r_5 - k_{deg,c3a} * C3a \quad (\text{S8})$$

$$\frac{dx_9}{dt} = r_3 + r_4 + r_5 - r_7 \quad (\text{S9})$$

$$\frac{dx_{10}}{dt} = r_6 - r_{10} - r_8 \quad (\text{S10})$$

$$\frac{dx_{11}}{dt} = r_7 - r_{11} - r_9 \quad (\text{S11})$$

$$\frac{dx_{12}}{dt} = r_{10} - r_{14} \quad (\text{S12})$$

$$\frac{dx_{13}}{dt} = r_{10} \quad (\text{S13})$$

$$\frac{dx_{14}}{dt} = -r_{12} - r_{13} \quad (\text{S14})$$

$$\frac{dx_{15}}{dt} = r_{12} + r_{13} - k_{deg,c5a} \quad (\text{S15})$$

$$\frac{dx_{16}}{dt} = r_{12} + r_{13} \quad (\text{S16})$$

$$\frac{dx_{17}}{dt} = -r_8 - r_{14} \quad (\text{S17})$$

$$\frac{dx_{18}}{dt} = -r_9 \quad (\text{S18})$$

$$(\text{S19})$$

585 where the rate equations are given by:

$$r_1 = \frac{k_{i1}(C4)}{(K_{1s} + C4)} \quad (\text{S20})$$

$$r_2 = \frac{k_2(C2)}{(K_{2s} + C2)} \quad (\text{S21})$$

$$f_1 = \frac{Zymo^{\eta_1}}{(Zymo^{\eta_1} + \alpha_1^{\eta_1})} \quad (\text{S22})$$

$$f_2 = \frac{Zymo^{\eta_2}}{(Zymo^{\eta_2} + \alpha_2^{\eta_2})} \quad (\text{S23})$$

$$r_3 = k_3(C3) \quad (\text{S24})$$

$$r_4 = \frac{k_4(C3C_L)(C3^{\eta_3})}{(K_{4s}^{\eta_3} + C3^{\eta_3})} \quad (\text{S25})$$

$$r_5 = \frac{k_5(C3C_A)(C3)}{(K_{5s} + C3)} \quad (\text{S26})$$

$$r_6 = k_6(C4b)(C2a) \quad (\text{S27})$$

$$r_7 = k_7(C4b)(C2a) \quad (\text{S28})$$

$$r_8 = k_8(C3C_L)(C4b)(C4BP) \quad (\text{S29})$$

$$r_9 = k_9(C3C_A)(FactorH) \quad (\text{S30})$$

$$r_{10} = k_{10}(C3C_L)(C3b) \quad (\text{S31})$$

$$r_{11} = k_{11}(C3C_A)(C3b) \quad (\text{S32})$$

$$r_{12} = \frac{k_{12}(C5C_L)(C5^{\eta_4})}{(K_{12s}^{\eta_4} + C5^{\eta_4})} \quad (\text{S33})$$

$$r_{13} = \frac{k_{13}(C5C_A)(C5)}{(K_{13s} + C5)} \quad (\text{S34})$$

$$r_{14} = k_{14}(C5C_L)(C4BP) \quad (\text{S35})$$